Backscatter differential phase. Estimation and variability.

S. Trömel[1], M. Kumjian[2], A. Ryzhkov[2], C. Simmer[3], A. Tokay[4], J.-B. Schroer[3]

[1] Hans-Ertel-Centre for Weather Research, Atmospheric Dynamics and Predictability Branch, University Bonn, Germany, silke.troemel@uni-bonn.de
[2] NOAA's National Severe Storms Laboratory, Norman, Oklahoma, USA, kumjian@ou.edu
[3] Meteorological Institute of the University of Bonn, Bonn, Germany, csimmer@uni-bonn.de
[4] Joint Center for Earth Systems Technology (JCET), University of Maryland Baltimore County (UMBC), Baltimore, Maryland, USA, Ali.Tokay-1@nasa.gov

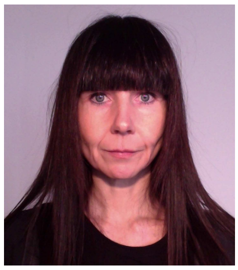

Silke Trömel

1. Introduction

Backscatter differential phase is one of the polarimetric variables which can be estimated from the measurements by dual-polarization weather radars. By definition, the backscatter differential phase δ is a difference between the phases of horizontally and vertically polarized components of the backscattered wave upon reflection from the scatterers within the radar resolution volume. It contributes to total differential phase Φ_{DP} along with "propagation differential phase" determined by radial profile of specific differential phase K_{DP} as

$$\Phi_{DP}(r) = \delta + 2\int_0^r K_{DP}(s)\,ds\,. \tag{1}$$

Hence, the contributions from the backscattered and propagation components of Φ_{DP} need to be separated before specific differential phase K_{DP} is estimated from the range derivative of Φ_{DP}. It was recognized relatively recently that accurate rainfall measurements using K_{DP} at X band are contingent on the effectiveness of such separation. Backscatter differential phase is significant for large hydrometeors of resonance sizes. Clear manifestations of noticeable differential phase in rain (at X and C bands) and in wet snow and melting hail (at X, C, and S bands) are frequently observed but no systematic studies of δ in various types of hydrometeors were performed so far.

One of the possible manifestations of the backscatter differential phase within the melting layer in stratiform precipitation is nonmonotonic radial profiles of Φ_{DP} through the melting layer. Zrnic et al. (1993) suggested that these are entirely related to δ and the magnitude of the Φ_{DP} excursion can be used for estimation of δ and dominant (or maximal) size of wet snowflakes within the melting layer. Ryzhkov and Zrnic (1998) and Ryzhkov (2007) provide alternative explanation of the perturbation of the Φ_{DP} profile and attribute at least part of it to the effects of nonuniform beam filling. The issue has to be clarified.

2. Backscatter differential phase in rain

2.1. Evidence of δ in rain at X band

As an example of observed δ in rain, Fig. 1 presents a genuine RHI taken along the 309.5° azimuth at 14:24 UTC on 22 June 2011 observed with the Polarimetric X band radar in Bonn, Germany (BoXPol). A prominent column of enhanced Z_{DR} is observed in the core of the cell (at a range of about 35 km). In this Z_{DR} column, Φ_{DP} values jump as high as 5° – 10° before returning to background values (0^0 – 4°) on the far side of the core. The region of large Φ_{DP} values located between 3 – 4 km in height and a range of 34.5 km is associated with contamination from side lobes and is not meteorological.

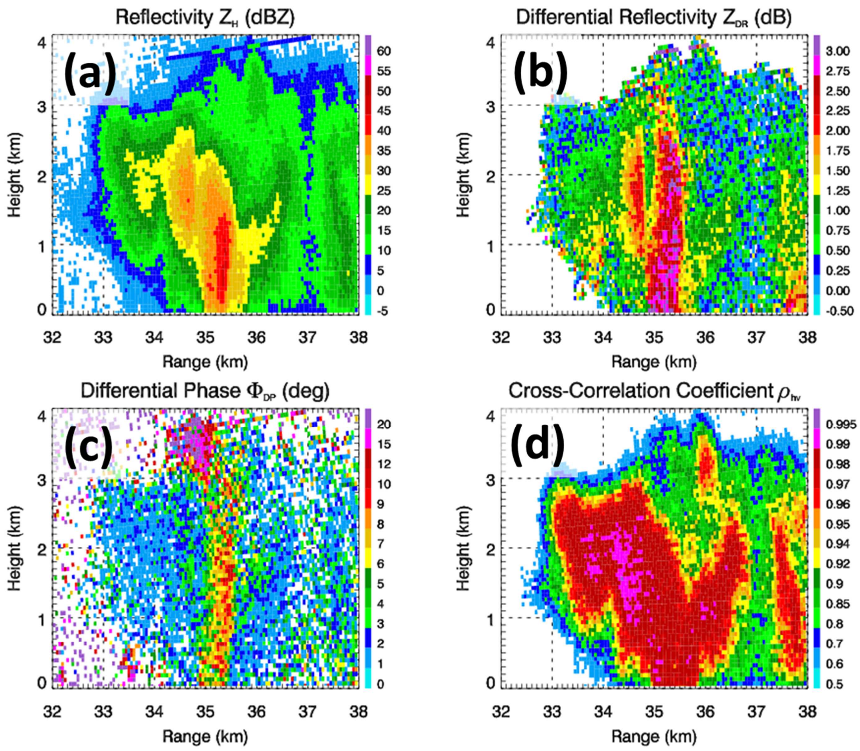

Fig. 1 Genuine RHI taken with 0.1° vertical resolution using BoXPol X-band radar on 06/22/2011. Evidence of differential phase upon backscattering in a column centered at about 35 km range from the radar.

2.2. Relation between δ and Z_{DR} at X band

Several measurements of drop size distributions (DSDs) as well as simulations using various DSD models confirm a strong interdependence between backscatter differential phase δ and differential reflectivity Z_{DR}. Otto and Russchenberg (2011) suggested the best fit relationship $\delta = Z_{DR}^{1.8}$ with δ in [°] and Z_{DR} in [dB] based on scattering computations at X band and a set of 1500 DSDs. Berne and Schneebeli (2012) confirm their results with a similar best fit power law: $\delta = 0.632\ Z_{DR}^{1.7}$. Generally, the authors claim that variability in Z_{DR}-δ relations predominantly stems from the different temperatures used in the simulations.

The impact of temperature on Z_{DR}-δ relationships is also clearly reflected in Fig. 2. 47144 DSDs measured with a 2D-Video Disdrometer (2DVD) in Oklahoma, USA, have been used to simulate Z_{DR} and δ at 0° and 30°C. Remarkable differences are recovered for the wide temperature range considered. It can be summarized that for higher temperatures, one has to expect larger exponents and significantly larger δ for a given Z_{DR}. In order to recover a possible impact of climatological differences in DSDs, simulations for 15°C are repeated using measurements from a Parsivel disdrometer in Bonn, Germany, covering the time period August 2007- January 2010. Simulations performed for 15°C show best agreement with the power law $\delta = Z_{DR}^{1.8}$ suggested by Otto and Russchenberg (2011) in the temperature range between 1 and 25°C. Fig. 2, however, clearly shows the consistency between Z_{DR}-δ relationships retrieved in Oklahoma and Bonn. The overwhelming part of variability can be related to the temperature of raindrops, the impact of differences in DSDs seems to be small.

Since Z_{DR} is affected by differential attenuation and sometimes biased due to miscalibration, the strong correlation between Z_{DR} and δ can be of interest for quantitative precipitation estimation (QPE). Fig. 3 shows the scatterplots of δ versus raindrop median volume diameter at 20°C simulated from the Oklahoma DSDs and δ versus mass-weighted average diameter at 15°C simulated from the DSDs measured in Bonn. Obviously, δ represents another useful parameter for characterizing drop sizes.

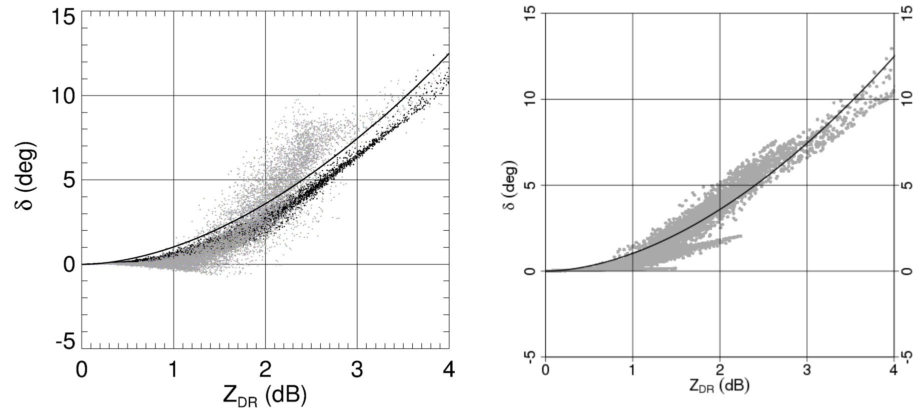

Fig. 2 Scatterplot of δ versus Z_{DR} in rain at X band as revealed from simulations using the Oklahoma disdrometer dataset (left). Black dots correspond to temperature 0° and grey dots are for temperature 30°. Solid line depicts the dependence $\delta = Z_{DR}^{1.8}$. A similar plot but from Parsival measurements in Bonn at 15°C (right) is shown for comparison.

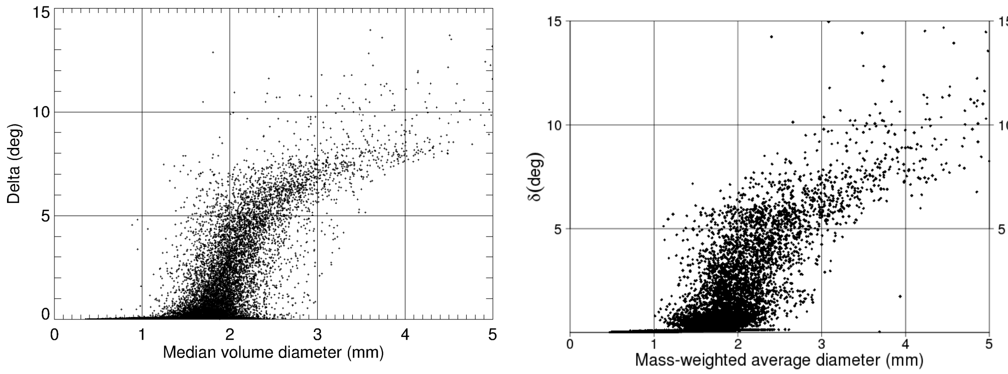

Fig. 3 The magnitude of δ versus median volume diameter for X band and T = 20°C based on DSD measurements in Oklahoma (left) and δ versus mass-weighted average diameter for X band and T=15°C based on DSD measurements in Bonn (right).

2.3. Estimation of δ in rain at X band

In this section, the combined application of the ZPHI-method (Testud et al., 2000) and the slightly modified self-consistent method with constraints proposed by Bringi et al. (2001) is suggested to determine δ in pure rain. Under the hypothesis of a power law relationship between the specific attenuation A and the unattenuated reflectivity Z

$$A = \beta Z^b \tag{2}$$

and a quasilinear relationship between specific attenuation and K_{DP}

$$A = \alpha K_{DP}^c \tag{3}$$

with constant parameters β, b, α, and c near unity in the considered range interval and an external constraint determined by a total span of measured Φ_{DP} along the ray, it is possible to derive the radial profile of specific attenuation A(r) from attenuated reflectivity $Z_a(r)$ using the ZPHI method. Once A(r) at each range is calculated according to the ZPHI algorithm a "calculated" radial profile of differential propagation phase φ_{DP} can be determined as

$$\varphi_{DP}^{cal}(r, \alpha; b) = 2\int_{r_1}^{r} \frac{A(s; \alpha; b)}{\alpha} ds. \tag{4}$$

Backscatter differential phase δ can be identified as the difference between measured Φ_{DP} and calculated φ_{DP} and using ρ_{HV}>0.9 as additional criterion for separating δ perturbations and the ones caused by noise or NBF.

In order to demonstrate the reliability of the method for δ detection, the spatial and temporal continuity of δ estimates is illustrated in Fig. 4. Fig. 4 shows PPIs of δ in two successive radar scans at 11:16 UTC and 11:21 UTC zoomed in the region of interest. Cells of δ can be identified and tracked over time, which demonstrates the spatial and temporal coherency of retrieved δ and attests to the reliability of its estimate. However, the method is less suitable for areas with high K_{DP}. Subtracting the estimated propagation component from measured differential phase profiles may result in accidental residuals if high gradients of Φ_{DP} prevail. It can be concluded that the method based on ZPHI provides reasonably robust estimates of δ and K_{DP} in pure rain where Φ_{DP} does not behave erratically as in the areas affected by NBF or low signal-to-noise ratios.

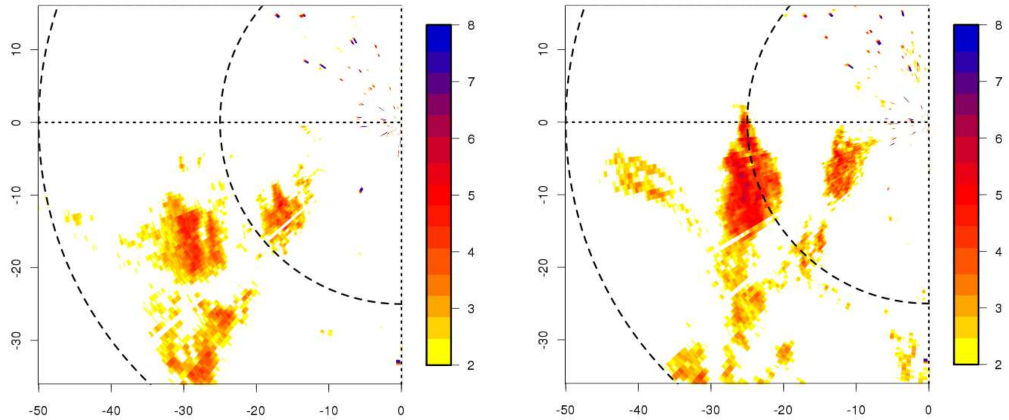

Fig. 4 PPIs of δ generated from observations on June 22, 2011 with BoXPol in 2 consecutive time steps at 11:16 UTC and 11:21UTC.

3. Backscatter differential phase within the melting layer

3.1. Variability of δ within the melting layer at X, C, and S bands

Differential phase Φ_{DP} routinely exhibits characteristic “bump” within the melting layer which may be associated with either backscatter differential phase δ or nonuniform beam filling (NBF). In order to suppress fluctuations of Φ_{DP} caused by reduction of ρ_{HV} within the melting layer, to separate effects of δ and K_{DP}, and to minimize the impact of NBF, azimuthally averaged radial profiles of Φ_{DP} from measurements at higher elevation angles are analyzed. Fig. 5 shows the azimuthally averaged profiles of Φ_{DP}, Z_{DR}, ρ_{HV}, and Z_H from the measurements on September 24, 2010 at 4:50 UTC with the polarimetric X-band radar in Jülich (JuXPol). The melting layer is clearly identified at around 2.2 km height showing an increase in Z_H and Z_{DR} and decrease of ρ_{HV}. The local increase of Φ_{DP} is almost exclusively attributed to δ. The maximum δ-value is about 7.5 degrees. Fig. 6 is an example of azimuthally averaged quasi-vertical profiles of the polarimetric radar variables measured by the C-band University of Oklahoma Polarimetric Radar for Innovations in Meteorology and Engineering (OU-PRIME; see Palmer et al. 2011). Again, the melting layer bright band is clearly observed in the vertical profiles of all four polarimetric radar variables. The maximal value of δ in this example exceeds 10°. At S band, the magnitiude of δ in the melting layer is expected to be smaller. Indeed, analyses of the polarimetric WSR-88D data near Seattle, Washington, USA (not shown here) reveal maximal δ within 3°.

Relative heights of different polarimetric moments and their magnitudes in the melting layer have been analysed for stratiform events in the area of the polarimetric twin-radars BoXPol and JuXPol. In the melting layer, the extrema for different moments occur at different heights. Maximum reflectivity Z_H is usually observed above the δ maximum, the maximum of δ may coincide with the ρ_{HV} minimum and both are above the Z_{DR} maximum. These relative heights of the extrema play an important role in understanding microphysics of the melting layer. Additionally, strong correlations between the extreme values of δ and Z_{DR} as well as between δ and ρ_{HV} have been observed in several cases (not shown here). Since the strength of the NBF effect should not depend on Z_{DR} or ρ_{HV} such correlations prove that δ estimates are reliable and the NBF effects are negligible.

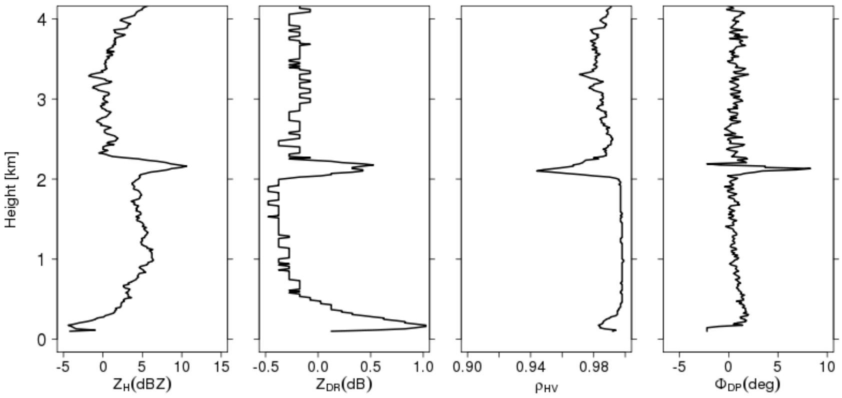

Fig. 5 Example of azimuthally averaged quasi-vertical profiles of Z_H, Z_{DR}, ρ_{HV}, and Φ_{DP} at X band.Data are obtained on 24 September 2010, at 4:50 UTC, from the PPI at elevation 37° by JuXPol in Jülich, Germany.

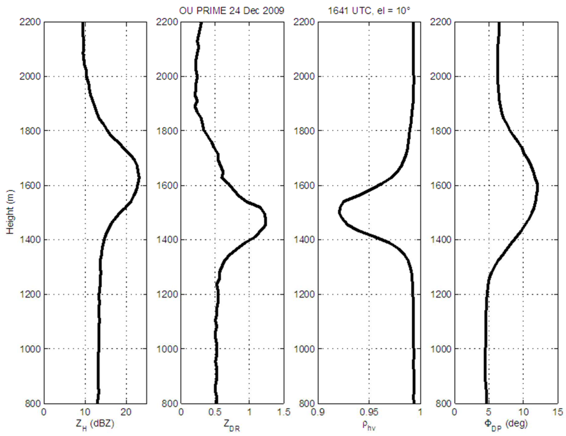

Fig. 6 Example of azimuthally averaged quasi-vertical profiles of Z_H, Z_{DR}, ρ_{HV}, and Φ_{DP} at C band. Data are obtained on 24 December 2009, at 16:41 UTC, from the PPI at elevation 10° by OU-PRIME in Norman, Oklahoma.

Berenguer and Zawadzki (2009) report clear correlation between the bright band intensity and Z_{DR} near the surface, i.e. big melting snowflakes make big raindrops. For light rain, K_{DP} may not be useful for rainfall estimation due to its noisiness and Z_{DR} can be biased by attenuation so that the $R(Z,Z_{DR})$ relations may be non-efficient as well. Thus, δ and Z_{DR} measurements and the analysis of their relationship in the melting layer may open a new avenue to parameterize Z-R-relationships to be utilized near the ground. For rimed snow, Z_{DR} and δ are lower (both in the melting layer and in rain below) and rain rate is higher for a given reflectivity Z_H as opposed to unrimed snow. Maybe the use of R(Z) relation parameterized by either Z_{DR} or δ is a promising alternative. Z_{DR} in the melting layer can be more sensitive to dominant size of precipitation particles than in pure rain near the surface where Z_{DR} changes weakly. Thus, rainfall estimation may benefit from quantification of different polarimetric variables in the melting layer. However, the full information content and benefit of the melting layer measurements for precipitation estimation and understanding the microphysics of precipitation processes has to be further explored. In some stratiform cases the correlations between between δ and ρ_{HV} is weaker. The δ-bumps are broader and especially the minima in ρ_{HV} are very flat and hard to identify.

4. Conclusions

Backscatter differential phase δ contributes to total differential phase Φ_{DP} along with propagation differential phase. For accurate rainfall measurements using K_{DP} at X band the contributions from the backscattered and propagation components of Φ_{DP} need to be separated before specific differential phase K_{DP} is estimated from the range derivative of Φ_{DP}. Backscatter differential phase is significant for large hydrometeors of resonance sizes.

New methods for estimating δ in rain and in the melting layer have been presented. The former is based on the ZPHI method and provides reasonably robust estimates of δ and K_{DP} in pure rain where Φ_{DP} does not behave erratically as in the areas affected by NBF or low signal-to-noise ratios. Several results of δ estimation in rain and melting layer using polarimetric radars operating at X, C, and S bands have been presented. One of the possible benefits of using δ is its direct relation to the prevalent size of hydrometeors so that δ can be used for more accurate retrieval of hydrometeor size distributions. Large disdrometer datasets collected in Oklahoma and Germany confirm a strong interdependence between backscatter differential phase δ and differential reflectivity Z_{DR}. The overwhelming part of variability can be related to the temperature of raindrops, whereas the impact of the differences in DSDs seems to be small. Since Z_{DR} is affected by differential attenuation and sometimes biased due to miscalibration, the strong correlation between Z_{DR} and δ is of interest for quantitative precipitation estimation (QPE). δ and Z_{DR} are differently affected by particle size spectra and can complement each other for particle size distribution (PSD) retrievals. The large disdrometer datasets have also been used to prove that δ may serve as another useful parameter for characterizing drop sizes.

Acknowledgement

This research was partly carried out in the Hans Ertel Centre for Weather Research. This research network of Universities, Research Institutes and the Deutscher Wetterdienst is funded by the BMVBS (Federal Ministry of Transport, Building and Urban Development). We gratefully acknowledge the support by the TERENO project (Terrestrial Environmental Observatories) funded by the Helmholtz-Gemeinschaft and the support by the SFB TR 32 (Transregional Collaborative Research Centre 32) funded by the DFG (German Research Foundation).

References

Berenguer M., and Zawadzki I., 2009: On the relationship between Z-R, the bright band intensity and Z_{DR}. *34th Conf. Radar Meteorol.*, Williamsburg, VA, 4A.3.

Bringi V. N., Keenan T. D., and Chandrasekar V., 2001: Correcting C-band radar reflectivity and differential reflectivity data for rain attenuation. A self-consistent method with constraints. *IEEE Trans. Geosci. Remote Sens.*, **39**, 1906-1915.

Otto T. and Ruschenberg H. W. J., 2011: Estimation of Specific Differential Phase and Differential Backscatter Phase From Polarimetric Weather Radar Mesurements of Rain. *IEEE Geoscience and Remote Sensing Letters*, **8(5),** 988-992

Palmer R. D., Bodine D., Kumjian M. R., Cheong B., Zhang G., Cao Q., Bluestein H. B., Ryzhkov A. V., Yu T.-Y., and Wang Y., 2011: Observations of the 10 May 2010 tornado outbreak using OU-PRIME: Potential for new science with high-resolution polarimetric radar. *Bull. Amer. Meteor. Soc.*, **92**, 871-891.

Park S.-G., Bringi V. N., Chandrasekar V., Maki M., Iwanami K., 2005: Correction of Radar Reflectivity and Differential Reflectivity for Rain Attenuation at X Band. Part I: Theoretical and Empirical Basis. *J. Atmos. Oceanic Technol.*, **22**, 1621-1632

Ryzhkov A. and Zrnic D., 1998: Beamwidth effects on the differential phase measurements of rain. *J. Atmos. Oceanic Technol.,* **15**, 624-634.

Ryzhkov A., 2007: The impact of beam broadening on the quality of radar polarimetric data. *J. Atmos. Oceanic Technol.*, **24**, 729 – 744.

Schneebeli M., and Berne A., 2012: An Extended Kalman Filter Framework for Polarimetric X-Band Weather Radar Data Processing. *J. Atmos. Oceanic Technol.,* **29**, 711–730.

Testud J., Le Bouar E., Obligis E., and Ali-Mehenni M., 2000: The Rain Profiling Algorithm Applied to Polarimetric Weather Radar. *J. Atmos. Oceanic Technol.*, **17**, 332-356.

Zrnic D., Balakrishnan N., Ziegler C., Bringi V., Aydin K., and Matejka T., 1993: Polarimetric signatures in the stratiform region of a mesoscale convective system. *J. Appl. Meteor.*, **32**, 678 – 693.